Isotopes and ion chemistry to identify salinization of coastal aquifers of Sabarmati River Basin

Kumari Rina[1], P. S. Datta[2], Chander Kumar Singh[1,3] and Saumitra Mukherjee[1,*]

[1]School of Environmental Sciences, Jawaharlal Nehru University, New Delhi 110 067, India
[2]Indian Agricultural Research Institute, New Delhi 110 012, India
[3]TERI University, Vasant Kunj Institutional Area, New Delhi 110 067, India

The lower reaches of the Sabarmati River Basin in Gujarat have intense agricultural and industrial activities and this part is affected by problems of groundwater salinity. Here we attempt to assess the processes governing the causes of groundwater salinity in the coastal alluvial aquifer, employing $\delta^{18}O$ and δD isotopes in integration with ionic ratio. The different hydrochemical facies such Na–Mg–HCO_3–Cl, Na–Cl–SO_4, Na–Mg–Cl–HCO_3–SO_4 and Na–Cl of groundwater show the occurrence of complex geochemical phenomenon in the study area. Ionic ratio (such as Mg^{2+}/Ca^{2+}, Na^+/Cl^-, SO_4^{2-}/Cl^-, K^+/Cl^-) and isotopic composition ($\delta^{18}O$ and δD) of groundwater indicate that while in coastal areas seawater intrusion is taking place, in inland areas various anthropogenic activities and overexploitation have induced salinity in groundwater. Over-pumping of groundwater has also induced lateral intermixing of highly saline water in the vicinity of coastal areas with relatively fresh/low saline groundwater along specific flow pathways.

Keywords: Coastal aquifers, groundwater salinization, ionic ratio, isotopic analysis, seawater intrusion.

GROUNDWATER resources in arid and semi-arid coastal areas are highly vulnerable to salinity problems from natural impacts like drought and seawater intrusion and by human influences like induced indiscriminate withdrawal of groundwater, leading to serious consequences on environment and economy of the region. The coastal area in the lower reaches of the Sabarmati River Basin in Gujarat is one such region having intense agricultural and industrial activities. In coastal areas of Gujarat, the problem of groundwater salinity was first detected in the late sixties and seventies after large-scale pumping by farmers. Over the years, the problem of salinity ingress has affected 12 coastal districts in the state. A total of 2542 villages are affected either by dynamic salinity or inherent salinity. It is a common assumption that the salinization of coastal aquifers is caused only by seawater intrusion as a result of over-pumping of groundwater, provided the hydraulic connection with sea exists. However, limited effort has been made in this context to understand the actual causes of groundwater salinization in this water-scarce region.

Besides seawater intrusion, alternative origins of groundwater salinization are also common from natural sources of mineral salts, evaporite dissolution, downward seepage from surficial saline water, return flows of irrigation with sewage effluent, deep brines or upward flow from deep saline water and fossil seawater[1–4]. The extent of saline water intrusion in any coastal area is influenced by the physico-chemical properties of the geological formations, sea to inland hydraulic gradient, and the rate of recharge and withdrawal of groundwater[5]. Groundwater salinization can also result from seepage of industrial and domestic waste water. The variations in sea level and changes in aquifer recharge control the processes at the interface between the freshwater and seawater. Changes in the interface position trigger dissolution–precipitation, ion exchange and redox reactions[6,7]. The $^2H(D)$ and ^{18}O stable isotopes are known to be potential markers of the water origin. Hydrochemistry when integrated with isotope hydrology offers a powerful tool to study the intermixing between water masses of different salinities and therefore help trace the source of saline water[8]. In the above background, the present study is an attempt to assess the processes governing the causes of groundwater salinity in the coastal alluvial aquifers of the lower reaches of the Sabarmati River Basin, Gujarat (Figure 1) during 2009–10.

Physiography, hydrogeology and climate of the study area

The study area (Figure 1) in the Sabarmati Basin merges into the coastal region of the Cambay Basin and is overlain with Quaternary alluvial and continental marine sediment deposits of fluvio-marine, fluvial and aeolian origin. During Holocene, the Gulf of Cambay was

*For correspondence. (e-mail: saumitramukherjee3@gmail.com)

connected with the Little Rann of Kachchh and a narrow strip of saline wasteland, with presence of evaporite and carbonates in the rocks, separates the western parts of Gujarat from the mainland. Sabarmati River and its major tributaries traverse across quartzites, phyllites, slates and schists in the upper reaches[9]. Sandy aquifer horizons laterally continuous and vertically interspersed with thin semipermeable clay/silt layers, are present towards the central and southern parts. Groundwater in all these formations occurs under unconfined to confined conditions. Since the tubewells tap all the horizons that yield water up to their maximum depth (450 m)[9], all the horizons are treated as a single regional aquifer unit and the individual sand layers as sub-aquifers, which are roughly inclined parallel to the ground surface.

Climate of the area in general is hot and dry except during the monsoon season. In summer, the maximum temperature remains about 42–44°C, whereas in winter the maximum temperature generally varies from 9 to 14°C. The average annual rainfall in the area[9,10] is about 600 mm, which is mainly influenced by the southwest monsoon that normally sets in the middle of June and continues to be active till mid-September. Monsoon rain contributes nearly 91–94% of annual precipitation. Due to scanty rainfall and an ephemeral river system, the entire study area depends heavily on groundwater for its domestic, agriculture and industrial requirements[9]. An acute shortage of water is exacerbated by the inferior water quality in terms of salinity.

Material and methods

Twenty groundwater samples from tube wells and bore wells were collected in March 2010 (representing both pre- and post-monsoon situation) from the coastal areas of some villages in the Sabarmati Basin in a part of Gulf of Cambay (Table 1). At each site water samples were collected in three separate, clean polypropylene bottles – one each for the anions, cations and isotopic analysis. The first few strokes of water were discarded to minimize the impact of iron pipes. For analysis of cations water samples were acidified, whereas for isotopic analyses a sealed aliquot of the sample was sent to the Physical Research Laboratory (PRL), Ahmedabad. pH, electrical conductivity (EC) and total dissolved solids (TDS) were measured onsite using respective electrodes (Hanna). The samples were stored in ice containing styrofoam boxes and kept in the laboratory at 4°C for further analysis.

The samples were vacuum filtered with 0.22 μm Millipore filter paper. Carbonate and bicarbonate were determined using titration method. Anions (F^-, Cl^-, SO_4^{2-} and NO_3^-) were analysed using ion chromatography (ICS-90, Dionex). Before analysis, the ion chromatograph was calibarated using Merck multielemental standard. Major cations (Ca^{2+}, Mg^{2+}, Na^+, K^+) were analysed using atomic absorption spectrophotometer (Thermo Fisher, M Series). The instrument was standardized using elemental standard (Merck). Dissolved silica was analysed by the molybdo-silicate method[11]. A total of 14 water quality parameters have been studied using graphical plots and statistical analyses. The isotopic analysis (δ^{18}O and δD) was done using standard equilibration method in which water samples (300 μl) are equilibrated with CO_2 and H_2. The equilibrated CO_2 and H_2 gases were analysed in Delta V Plus isotope ratio mass spectrometer in continuous flow mode using GasBench II for $^{18}O/^{16}O$ and D/H ratios. The reproducibility of the measurement[12] was better than 0.1‰ for δ^{18}O and 1‰ for δD. The δ^{18}O and δD values obtained in the laboratory were corrected using an integrated calibration curve based on VSMOW2, GISP and SLAP2 (obtained from International Atomic Energy Agency, Vienna) measurements. The calibration equations used for the reported values are

$$\delta^{18}\mathrm{O}_{(\mathrm{corrected})} = 1.0025(\pm 0.0009) \times \delta^{18}\mathrm{O}_{(\mathrm{measured})} + 0.0156(\pm 0.0302),$$

and

$$\delta\mathrm{D}_{(\mathrm{corrected})} = 1.0025(\pm 0.0006) \times \delta\mathrm{D}_{(\mathrm{measured})} + 0.0044(\pm 0.1710).$$

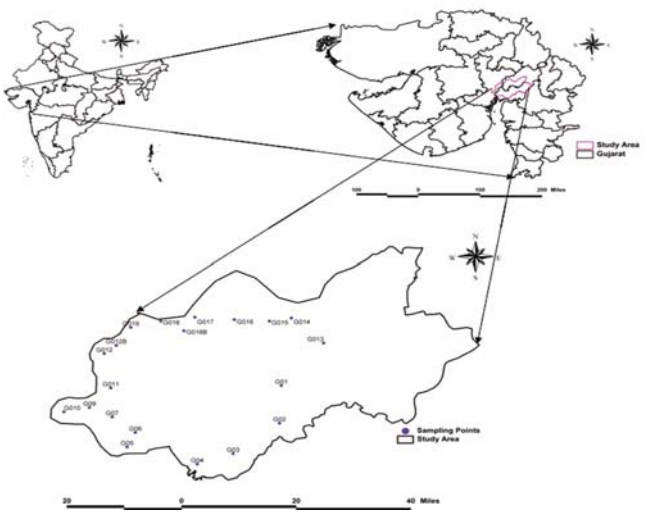

Figure 1. Map showing the study area with sampling locations.

Results and discussion

Details of the chemical analysis of groundwater are given in Table 1. Groundwater of the studied area is alkaline in nature, with an average pH of 8.42. EC ranged from 750 to 3,820 μS/cm with 2,352 μS/cm average, whereas

Table1. Details of water quality parameters analysed (concentration in mg/l, except EC (µS/cm) and pH)

Sampling locations	Samples	pH	Electrical conductivity	Total dissolved solids	CO_3	HCO_3	F	Cl	NO_3	SO_4	SiO_2	Na	K	Ca	Mg	$\delta^{18}O$	δD
Piplau Ashapuri	G01	8.1	2046	1310	60	646.6	2.34	321.87	51.18	49.37	87.53	353.6	2.34	5.06	74.31	–2.37	–15.74
Jogan Telpura	G02	8.1	765	490	60	292.8	0.6	36.52	33.87	18.41	67.92	48.33	0.97	30.40	76.41	–2.39	–17.22
Vadola	G03	7.7	3350	2150	12	585.6	1.11	527.06	122.46	95.02	133.22	421.2	7.20	15.94	168.14	–2.36	–15.04
Hirapur	G04	8.4	3450	2210	24	549	0.52	794.79	49.89	611.45	137.47	536.25	17.30	83.20	148.08	–2.20	–14.68
Pandal	G05	8.3	3360	2150	52	402.6	4.98	737.28	1346.42	734.86	132.00	375.53	256.39	41.38	291.82	0.55	–1.39
Rohini	G06	8.6	843	540	72	244	1.46	72.46	40.09	24.1	48.43	73.36	26.25	19.22	53.61	–3.17	–28.56
Golana	G07	7.9	2420	1550	24	512.4	0.66	428.73	3.06	106.6	68.44	146.15	33.13	24.89	111.78	–1.89	–17.19
Naniboru	G09	8.4	3510	2250	48	353.8	0.92	884.94	17.53	705.06	54.48	804.74	59.05	51.96	102.87	0.34	–2.74
Naniboru	G10	8.4	3560	2280	36	658.8	0.86	1388.94	2223.75	1325.44	76.87	1288.09	19.71	30.08	322.81	0.15	–1.22
Vataman	G11	8.6	750	480	24	109.8	0.51	115.81	75.02	44.89	26.88	76.83	16.75	17.29	51.46	–2.68	–29.05
Simej	G12	8.4	3820	2450	24	383.8	0.79	537.77	10.47	429.88	49.71	361.2	9.25	25.14	72.52	–2.69	–17.20
Simej	G12B	8.7	3670	2350	36	305	0.44	519.42	4.02	441.18	48.79	521	5.94	56.47	54.5	–3.06	–20.40
Guntal	G13	8.4	1980	1270	60	439.2	0.42	341.35	94.27	84.91	116.59	154.21	1.37	20.04	107.34	–2.72	–16.85
Dhaban	G14	8.9	1220	780	96	561.2	1.66	54.15	25.64	33.57	98.50	263.3	4.10	4.92	16.79	–2.22	–18.15
Palana	G15	8.4	1160	730	60	427	1.06	81.7	26.11	33.89	59.90	187.62	1.46	21.83	51.02	–2.37	–18.66
Matar	G16	8.7	1780	1140	46	532	2.82	129.12	24.08	74.58	65.27	142.8	4.90	1.94	76.79	–2.46	–16.60
Chandana	G17	8.6	3400	2240	36	475.8	1.79	544.66	46.53	323.43	52.99	326.31	2.14	18.38	104.26	–2.00	–14.15
Rasikpura	G18	8.7	1680	1250	72	488	1	80.36	7.99	63.21	50.12	105.66	1.60	32.48	84.64	–3.18	–20.71
Rasikpura	G18B	8.6	2390	1530	42	475.8	1.02	389.17	10.49	262.09	53.39	222.9	1.91	37.45	92.61	–2.60	–17.04
Near IBP Ahmedabad	G19	8.6	1890	1210	48	329.4	0.48	322.67	5.02	208.8	55.21	344.02	5.17	32.92	45.07	–2.98	–18.75

TDS ranged from 480 to 2,450 mg/l with 1,518 mg/l average. The degree of salinization in a given area can be indicated by an increase in TDS and possibly an increase in all cations and anions. The abundance of major anions in the study area is $HCO_3^- > Cl^- > SO_4^{2-} > NO_3^-$. Concentration of chloride ranged from 36.52 to 1,388.94 mg/l with 415.44 mg/l average, whereas sulphate concentration ranged from 18.41 to 1,325.44 mg/l with 283.54 mg/l average. The abundance of cations is in the order: $Na^+ > Mg^{2+} > Ca^{2+} > K^+$. The average concentration of sodium was 337.66 mg/l, whereas average concentration of Mg was 105.34 mg/l. The fluoride levels varied from 0.42 to 4.98 mg/l with average concentration 1.27 mg/l. Some samples show high concentration of NO_3^-. At some places, concentration of both fluoride (e.g. at sampling location G01, G03, G05, G06, G14, G16, G17) and nitrate (e.g. at sampling location G01, G03, G04, G05, G10, G11, G13, G17) is higher than the permissible limit in drinking water suggested by the Bureau of Indian Standards[13] and World Health Organization[14]. Most of the parameters vary in wide ranges with high standard deviations, perhaps due to local effects, suggesting multiple sources of contamination, influence of complex hydrochemical process and significant deterioration of groundwater quality in the study area.

Correlation of physicochemical parameters of groundwater

To show the degree of dependency of one variable to the other, correlation coefficient has been used. Prior to statistical analysis, the data were standardized with the criterion presented by Davis[15]. Both EC and TDS are strongly correlated with Cl^-, SO_4^-, Na^+, Ca^{2+} and Mg^{2+}. Na^+ and Mg^{2+} are also strongly correlated with chloride and sulphate. Very high correlation between Na^+ and Cl^- ($r^2 = 0.914$) indicates presence of highly saline water in the study area. In general, most ions are positively correlated with Cl^-, especially Na^+, Mg^{2+} and SO_4^{2-}, which indicates that such ions are derived from the same source. K^+ and F^- showed good correlation with each other, which suggests that these ions have been possibly contributed by the presence of K-feldspar, plagioclase, biotite, fluorite and apatite-bearing minerals in the study area. Mg^{2+} showed significant correlation with sulphate ($r^2 = 0.775$) and nitrate ($r^2 = 0.887$). Good correlation was observed for Cl^-–NO_3^-, Cl^-–SO_4^-, K^-–NO_3^-, Mg^-–NO_3^-, and NO_3^-–SO_4^{2-}, which suggests possible impact of leaching of excess fertilizers used for agricultural activity, that may create a long-term risk of groundwater pollution, as observed in an earlier study[16]. The positive correlation between Ca^{2+} and SO_4^{2-} suggests that besides the dissolution of anhydrite and/or gypsum, anthropogenic activity is also responsible for the presence of these ions in groundwater. Correlation of different water quality parameters is given in Table 2.

Identification of geochemical process

Statistical analysis of the data indicates that significant correlation exists between the total cation (TZ^+) and total anions (TZ^-; Figure 2) by the following relationship

$$TZ^- = 1.3093TZ^+ - 3.5667, \text{ with } R^2 \text{ value of } 0.9577.$$

The $(Ca^{2+} + Mg^{2+})$ versus $(HCO_3^- + SO_4^{2-})$ scatter diagram (Figure 3) shows that more samples are distributed above the equiline (1 : 1). This indicates that carbonate weathering is more prominent in the study area, although silicate weathering is also taking place[17,18]. Since the chemical composition of groundwater in coastal aquifers depends largely on the hydrochemistry of the freshwater component, which is intimately linked to the geology of the recharge areas, it is important to understand the relationships between saline water and the surrounding freshwater. Each potential source of salinization can be characterized by a distinguishable chemistry and well-known ionic ratio (Table 3) associated with different geochemical processes (e.g. $Mg^{2+}/Ca^{2+} > 5$: seawater intrusion) as mentioned in Table 3 with supported references[19–22].

In general, freshwater is dominated by calcium and seawater by magnesium; the Mg^{2+}/Ca^{2+} ratio can provide an indicator of seawater intrusion[23]. Mg^{2+}/Ca^{2+} ratio greater than 5 is a direct indicator of seawater

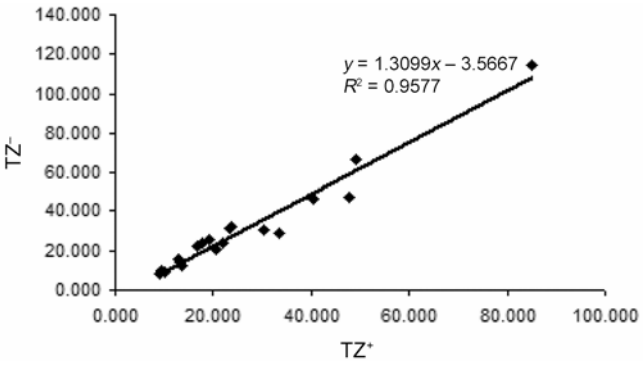

Figure 2. Plot showing relationship between total cation and total anion.

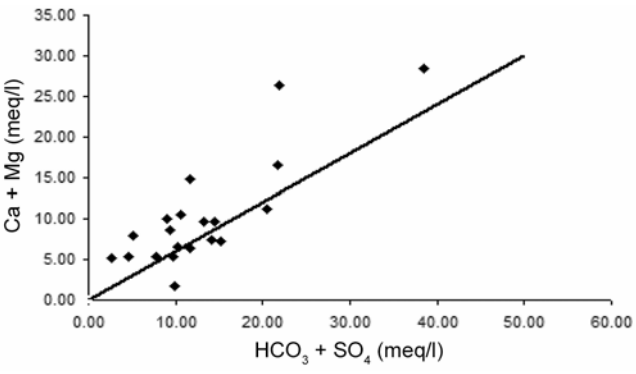

Figure 3. Scatter diagram of $(Ca^{2+} + Mg^{2+})$ versus $(HCO_3^- + SO_4^{2-})$.

Table 2. Correlation of different water quality parameters

	pH	EC	TDS	CO_3	HCO_3	F	Cl	NO_3	SO_4	SiO_2	Na	K	Ca	Mg
pH	1													
EC	–0.216	1.000												
TDS	–0.202	0.998	1.000											
CO_3	0.467	–0.581	–0.569	1.000										
HCO_3	–0.261	0.354	0.360	0.009	1.000									
F	0.006	0.089	0.088	0.232	0.209	1.000								
Cl	–0.226	0.830	0.820	–0.485	0.363	0.039	1.000							
NO_3	–0.094	0.343	0.337	–0.087	0.300	0.344	0.696	1.000						
SO_4	0.004	0.720	0.713	–0.315	0.237	0.113	0.942	0.788	1.000					
SiO_2	–0.433	0.296	0.284	–0.038	0.535	0.338	0.299	0.267	0.178	1.000				
Na	–0.076	0.687	0.677	–0.283	0.391	–0.054	0.914	0.684	0.903	0.179	1.000			
K	–0.139	0.275	0.268	0.008	–0.103	0.748	0.322	0.491	0.401	0.374	0.131	1.000		
Ca	0.020	0.493	0.494	–0.306	–0.138	–0.234	0.491	0.085	0.524	0.176	0.380	0.235	1.000	
Mg	–0.365	0.552	0.549	–0.322	0.399	0.386	0.788	0.887	0.775	0.508	0.639	0.592	0.260	1.000

Table 3. Ionic ratio of sampling points

Sample	Mg/Ca	Na/Cl	SO_4/Cl	K/Cl
G01	24.47	1.70	0.11	0.007
G02	4.19	2.04	0.37	0.024
G03	17.58	1.23	0.13	0.012
G04	2.97	1.04	0.57	0.020
G05	11.75	0.79	0.74	0.317
G06	4.65	1.56	0.25	0.330
G07	7.48	0.53	0.18	0.070
G09	3.30	1.40	0.59	0.061
G10	17.89	1.43	0.71	0.013
G11	4.96	1.02	0.29	0.132
G12	4.81	1.04	0.59	0.016
G12B	1.61	1.55	0.63	0.010
G13	8.93	0.70	0.18	0.004
G14	5.69	7.51	0.46	0.069
G15	3.89	3.54	0.31	0.016
G16	65.92	1.71	0.43	0.035
G17	9.45	0.92	0.44	0.004
G18	4.34	2.03	0.58	0.018
G18B	4.12	0.88	0.50	0.004
G19	2.28	1.65	0.48	0.015

Table 4. Ionic ratio given by different authors

Parameter	Seawater intrusion	Deep saline upcoming	Agriculture return flow	Wastewater infilteration
Na^+/Cl^-	0.86–1[19]	< 0.8[20]	–	1.1[3]
SO_4^{2-}/Cl^-	0.05[3,19]	~ 0.05[3,20]	≫ 0.05[21]	0.09[3]
K^+/Cl^-	0.019	< 0.019[3]	–	≫ 0.02
Mg^{2+}/Ca^{2+}	>5[20,22]	> 1[19]	–	–

contamination[20,22]. Likewise, seawater and seawater diluted with freshwater have distinguished geochemical characteristics[22,24]. At sampling location G01, G03, G05, G07, G010, G013, G014, G016 and G017 Mg^{2+}/Ca^2 ionic ratio was 5 or > 5 which shows the possibilities of direct contamination by seawater. However, with G013, G016 and G017 being located far away from the coast, direct contamination by seawater can be ruled out. In the other sampling locations, the ratio > 1 suggests possibilities of deep brine upconing.

In seawater, sodium and chloride are the other dominant ions. Thus high levels of Na^+ and Cl^- ions in adjacent coastal groundwater may indicate a significant effect of seawater mixing, in addition to dissolution of saline rock beds. A linear relation between Na^+ and Cl^- represents simple mixing of the fresh groundwater with the seawater. The Na^+/Cl^- ratios 0.8–1.0 at sampling locations G04, G011, G012, G017 and G018B indicate seawater intrusion with G017 and G018B being located far away from the coast, direct contamination by seawater can be ruled out. At sampling locations G05, G07 and G013 Na^+/Cl^- ratio is < 0.8, which shows possibilities of deep brine upconing. The ionic ratios of $SO_4^{2-}/Cl^- > 0.05$ in most of the locations indicate contamination from anthropogenic sources as well. A high SO_4^{2-}/Cl^- ratio is attributed to the application of gypsum fertilizers[21]. Ionic ratio of $K^+/Cl^- = 0.019$ indicates seawater intrusion. At sampling locations G01, G03, G010, G012, GO12B, G013, G015, G017, G018, G018B and G019, ionic ratio of K^+/Cl^- indicates possibilities of deep saline water upcoming. At sampling locations G02, G04, G05, G06, G07, G09, G011, G014 and G016, ionic ratio of $K^+/Cl^- \gg 0.02$ indicates wastewater infiltration. The ionic ratio of groundwater has almost become similar to seawater due to prolonged abstraction of groundwater.

The salinization problem is related to natural recharge mechanisms and that seawater intrusion has a more local influence and must be considered as a process induced by overexploitation of water resources that exacerbates the deterioration of groundwater quality. From the elevation contour map of the area (Figure 4), it is clear that elevation is higher in the central and eastern parts and it decreases towards the southwestern part. Topographically, sampling points G01, G013, G015, G016 and G017 lie at a higher elevation than G03, G04, G05, G06 and G011. A comparison of the chloride contour map (Figure 5) with the elevation contour map (Figure 4) of the area indicates that high elevation points have relatively low chloride content, and freshwater and groundwater salinity

is relatively higher in low elevation area. Elevation gradient is almost the same at G012 and G012B and near high saline area at G03 and G04.

In any natural condition, the groundwater usually follows the pattern of surface topography in the area. From the water table contour maps (Figure 6), it is clear that there is not much change in the hydraulic gradient in pre-monsoon (January 2009), monsoon (August 2009) and post-monsoon (November 2009), and the hydraulic gradient of the groundwater flow is from the central part towards the coast. Throughout the studied area there is lowering of groundwater table from August 2009 to November 2009 possibly induced by over-pumping. In sampling point G05 and G06, the water table was 4 mbgl in January 2009 which became 5 mbgl in November 2009. From pre- to post-monsoon, due to further decline in groundwater level, it is quite likely that hydraulic gradient changed from sea to inland area. Similar condition was found in G03–G04 and G09–G010. The lowering of the water table from groundwater abstraction might have induced a change in gradient from sea to inner land at these points. Near the coastal region, water table gradient declining is higher between G05–G06–G07 and G09–G010 at a short distance, which suggests increased withdrawal activity of groundwater. If over-withdrawal of groundwater is continued, the situation of salinity increase in groundwater is likely to worsen in the near future.

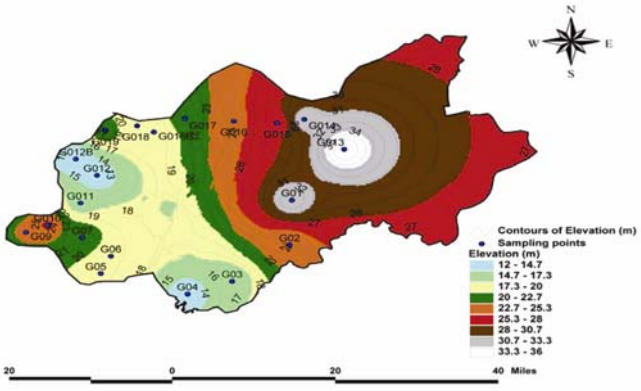

Figure 4. Elevation map of the area.

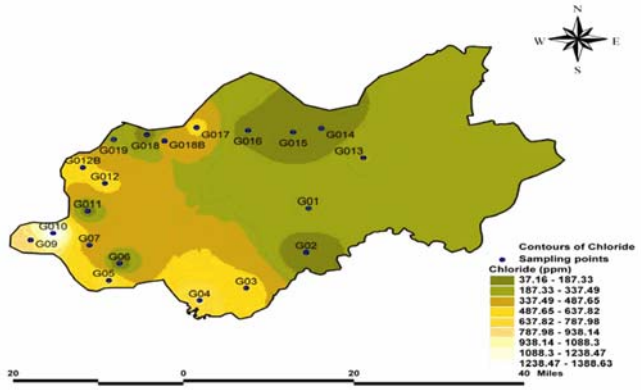

Figure 5. Spatial variation of chloride.

Origin of water

The water stable isotope content is a marker of the water origin. When combined with the water ionic content, it offers a powerful tool to study the mixing between water masses of different salinities and therefore to trace back the salinity origin[8]. Oxygen-18 and deuterium (^{2}H) data were used to assess the genesis and evolution of groundwater. The relationship trend between δ^2H and δ^{18}O (Figure 7) was compared with the equation of local meteoric water line (LMWL) calculated from the following relation for North Gujarat[25].

$$\delta D = (7.6 \pm 0.6) * \delta^{18}O - (2.9 \pm 2.2)\ [R^2 = 0.89].$$

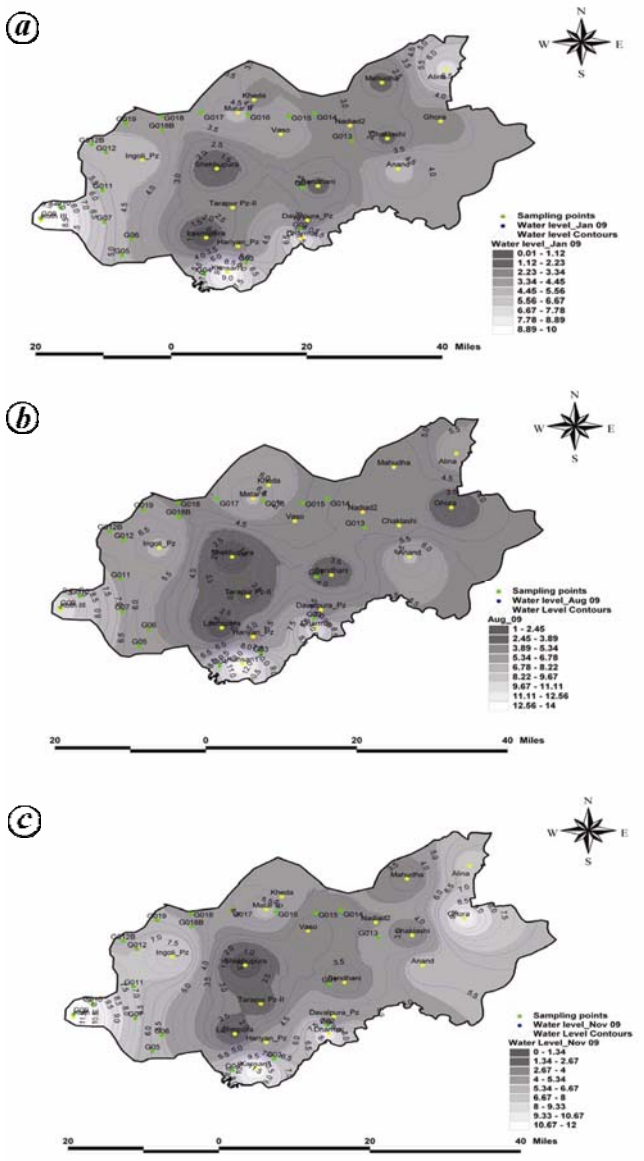

Figure 6. Water level contour maps. ***a***, January 2009; ***b***, August 2009; ***c***, November 2009.

The slope of LMWL is less than the slope of the Global Meteoric Water Line (GMWL) (8.17), yet, almost comparable with it. However, the intercept of LWML is significantly less than that of GMWL. This indicates considerable evaporation of rainwater during its fall. It was found that most of the groundwater samples fall along LMWL, but five samples deviated from LMWL. Among these, three on the top (samples G05, G09 and G010) were less deviated compared to two samples (G06 and G011) at the bottom. The deviation of the points G05, G09 and G010 is not much from LMWL, suggesting that the groundwater originated from local precipitation with possibility of evaporative enrichment. The evaporative enrichment is more in sample numbers G06 and G011 compared to G05, G09 and G010. These points which have highly saline water are also enriched in δ^{18}O value, while at other points δ^{18}O composition is relatively depleted with the value of –2.71 to –3.1. From the δ^{18}O contour map (Figure 8) it can be seen that a very high gradient exists within a small distance of 2 km from G010 to G011, G010 to G07 and from G06 to G05, suggesting that some impervious boundary is present in the geological formation at these points. Because of the presence of the impervious boundary, lateral mixing of groundwater does not occur.

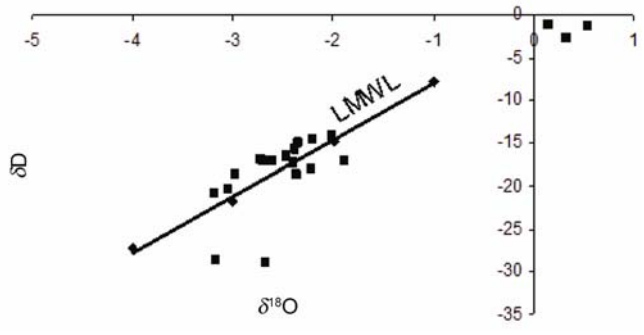

Figure 7. Relationship between δ^{2}H and δ^{18}O.

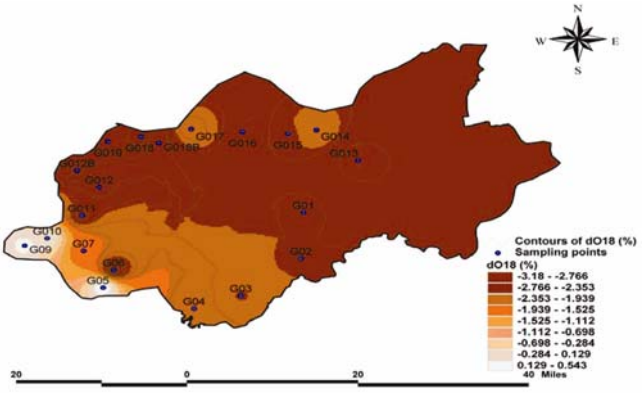

Figure 8. Contour map of δ^{18}O.

Relationship of Cl and δ^{18}O

Figure 9 shows that sample points G05, G09 and G010 (with high chloride content) have highly enriched δ^{18}O values, which indicates the possibilities of evaporative isotopic enrichment. It is also clear from Figure 9 that there is no change in δ^{18}O when there is an increase in chloride content. It may be due to leaching of Cl from land surface.

Intermixing of highly saline water with relatively fresh groundwater can be visualized along different specific flow pathways induced by pumping (Figure 9). For example, in the plot of δ^{18}O versus Cl (Figure 10), the points G09, G07, G011 and G06 fall along a straight line suggesting that there is intermixing of groundwater along specific pathways. One mixing line can also be visualized between G03, G04, G013 and G06. Sampling points G05 and G06 are nearby, but no mixing takes place as is evident from both ionic and isotopic ratios. This is due to the presence of impervious geological barrier between these two points, which is clear from the high isotopic gradient between the two in a short distance. G06 being located in the vicinity of the river, groundwater salinity at that point can come from nearby rivulets due to hydraulic gradient from river to adjacent inland. High chloride content in G03 and G04 may be due to sea-water ingression through nearby rivers and rivulets and subsequent intermixing due to groundwater withdrawal.

The ionic ratio of groundwater for the sampling point G05 shows that Mg^{+}/Ca^{2+} = 11.75 and Na^{+}/Cl^{-} = 0.786,

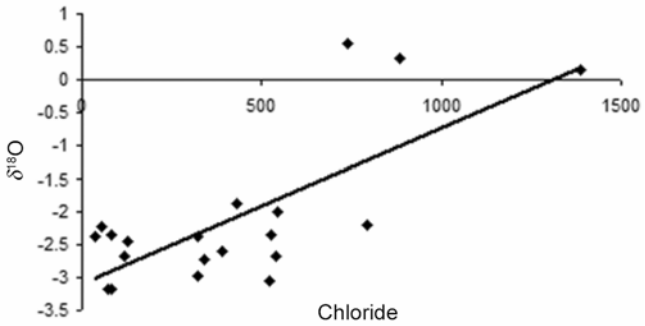

Figure 9. Scatter plot of Cl versus δ^{18}O.

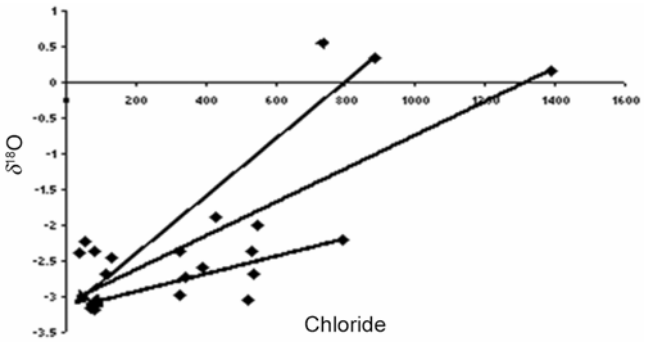

Figure 10. Cl versus δ^{18}O showing different flowing pathways.

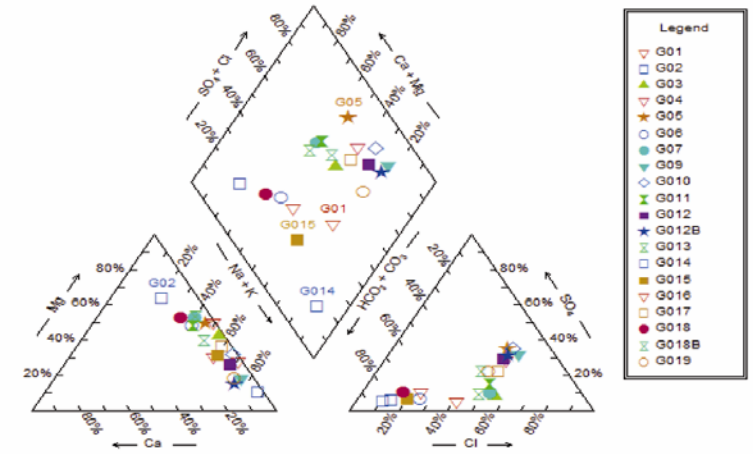

Figure 11. Piper diagram.

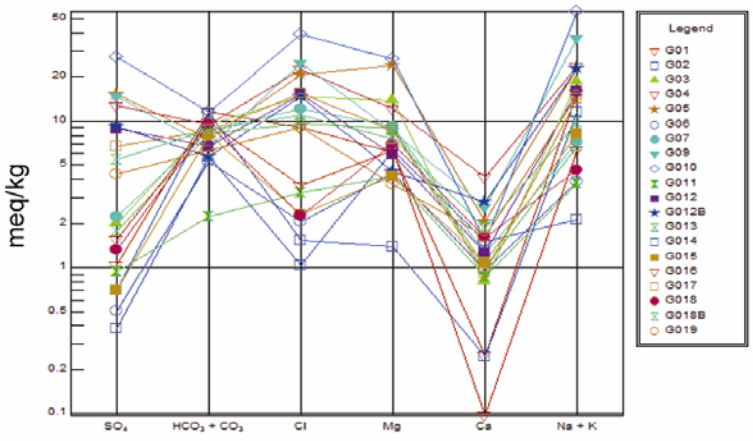

Figure 12. Schoeller diagram.

which is similar to that of seawater, suggesting the possibilities of intrusion. For G09, Mg^{2+}/Ca^{2+} = 3.299, showing deep brine upconing and Na^{+}/Cl^{-} = 1.404, showing wastewater infiltration. For G010, Mg^{2+}/Ca^{2+} = 17.887 and Na^{+}/Cl^{-} = 1.431, which again shows salinity due to wastewater infiltration. Radiocarbon age of groundwater of this area is 35,000 years BP in the western part and between 2,000 and 10,000 years BP in other parts of the studied area[26] around the Sabarmati Basin, suggesting that the groundwater got recharged in the past during humid conditions and subsequently became saline due to anthropogenic activities.

Geochemical classification

Piper trilinear diagram[27] (Figure 11) and Schoeller[28] diagram (Figure 12) have been used to understand the hydrochemical process operating in the groundwater system. The diagrams show that among cations, Na^{+}, K^{+} and Mg^{2+} are dominant and among anions, HCO_3^{-}, Cl^{-} and SO_4^{2-} are dominant. Some samples show Na–Mg–HCO_3–Cl facies, some Na–Cl–SO_4 facies and others Na–Mg–Cl–HCO_3–SO_4. The bicarbonate facies characterizes principally freshwater and the chloride facies characterizes a mixture with seawater. Variation in the cation composition is perhaps more difficult to analyse, because of the influence of three factors, namely (i) characteristics of freshwater, (ii) seawater intrusion and (iii) secondary processes such as cation exchange. The ion exchange reaction of Na^{+} and Ca^{2+} often occurs when seawater intrudes freshwater. When seawater intrudes a freshwater aquifer the following ionic exchange reactions represent cationic behaviour[29]:

$$2Na^{+}\,(K^{+}) + Ca - X_2 = 2Na(K^{+}) - X + Ca^{2+},$$

$$2Na^{+}\,(K^{+}) + Mg - X_2 = 2Na(K^{+}) - X + Mg^{2+},$$

where X represents ion exchange sites in aquifer material. When freshwater flushes out saline groundwater, the reverse reactions occur. It would not be out of point to mention here that even deep brines may have high

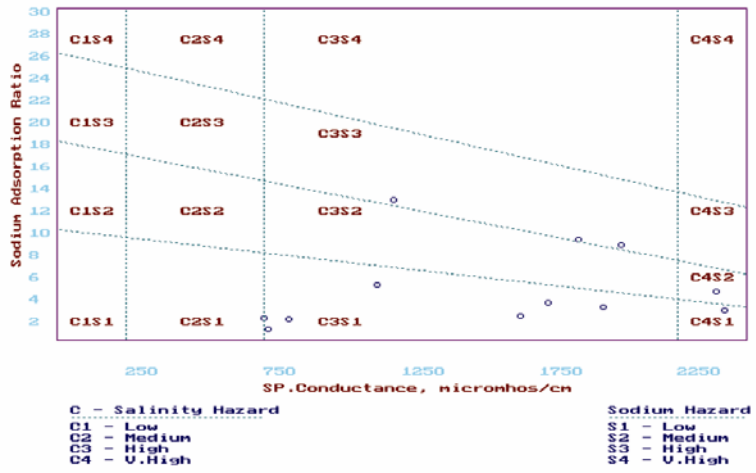

Figure 13. The United States Salinity Laboratory diagram of the area.

calcium (Ca^{2+}) content caused by base exchange reactions with clay minerals and dissolution of carbonate minerals[19]. The increase of Na^+ and Cl^- ions may indicate a significant effect of seawater mixing, while considerable amount of HCO_3^- and Ca^{2+} reflects water–rock interaction. The samples showing similar pattern in Schoeller[28] suggest possibilities of lateral intermixing of highly saline and fresh groundwater among these points.

Salinity hazard

EC and Na^+, HCO_3^- and CO_3 play a vital role in suitability of water for irrigation. Higher concentration of these salts causes changes in soil structure, permeability and aeration which indirectly affect the plant growth[30,31]. EC is a measure of salinity hazard as it reflects the content of TDS in groundwater. The US Salinity Laboratory Staff[32] proposed irrigational specifications for evaluating the suitability of water for irrigation use. The values of EC and sodium adsorption ratio when plotted (Figure 13) show that at most places groundwater of the area belongs to C3S1 category (high salinity and low alkalinity). This is considered as a suitable class for agricultural purposes. Some samples fall under C3S3 category. Very few samples fall under C4S1 and C4S2 category, which is a poor zone of water quality.

It has been observed from the different ionic ratios and from the isotopic data that the area has been affected by high salinity in groundwater (Figure 13). However, Na% is not very high and the groundwater is suitable for irrigation purpose. But, if overexploitation of groundwater is continued, the situation is likely to get aggravated, especially in the areas near the coast.

Conclusion

Three principal mechanisms seem to be taking place: recharge by freshwater (related mainly to weathering of different silicates), mixing with seawater and secondary reactions such as cation exchange. The present study suggests that groundwater chemistry in the study area is largely determined by the first of these processes, i.e. the lateral recharge flows, which introduce water with a different chemical composition than the rocks they flow through. In turn, this variability of freshwater recharge causes the chemistry of the groundwater in the aquifers to vary widely, as a result of intermixing between two or more water types. This situation is even more complicated when seawater participates due to intrusion, because the mixing process can follow diverse evolution trends. Moreover, when this process occurs, the participation of base exchange reactions is also recognized; principally reverse cation exchange in more salinized waters. The salinization problem is related to natural recharge mechanisms and seawater intrusion has a more local influence induced by overexploitation of groundwater resources.

1. Pulido-Leboeuf, P., Pulido-Bosch, A., Calvache, M. L., Vallejos, A. and Andreu, J. M., Strontium, SO_4^{2-}/Cl^- and Mg^{2+}/Ca^{2+} ratios as tracers for the evolution of seawater into coastal aquifers: the example of Castell de Ferro aquifer (SE Spain). *C.R. Geosci.*, 2003, **335**, 1039–1048.
2. Aunay, B., Dörfliger, N., Duvail, C., Grelot, F., Le Strat, P., Montginoul, M. and Rinaudo, J.-D., Hydro-socio-economic implications for water management strategies: the case of Roussillon coastal aquifer. In International Symposium-DARCY. Aquifer Systems Management, Dijon, 2006.
3. Vengosh, A., Spivack, A. J., Artzi, Y. and Ayalon, A., Geochemical and boron, strontium, and oxygen isotopic constraints on the origin of the salinity in groundwater from the Mediterranean coast of Israel. *Water Resour. Res.*, 1999, **35**, 1877–1894.
4. Yamanaka, M. and Kumagai, Y., Sulfur isotope constraint on the provenance of salinity in a confined aquifer system of the southwestern Nobi Plain, central Japan. *J. Hydrol.*, 2006, **325**, 35–55.
5. Freeze, R. A. and Cherry, J. A., *Groundwater*, Prentice Hall, NJ, 1979, p. 604.
6. Appelo, C. A. J., Cation and proton exchange, pH variations and carbonate reactions in a freshening aquifer. *Water Resour. Res.*, 1994, **30**, 2793–2805.

7. Appelo, C. A. J., Multicomponent ion exchange and chromatography in natural systems. *Rev. Mineral*., 1996, **34**, 193–227.
8. Fritz, P. and Fontes, J.-Ch. (eds), *Handbook of Environmental Isotope Geochemistry. Vol. 1, The Terrestrial Environment*, Elsevier, Amsterdam, 1980.
9. Gupta, S. K., Deshpande, R. D., Agrawal, M. and Raval, B. R., Origin of high fluoride in groundwater in the North Gujarat–Cambay region, India. *Hydrogeol. J*., 2005, **13**, 596–605.
10. Datta, P. S., Desai, D. I. and Gupta, S. K., Hydrological investigations in Sabarmati basin. I. Groundwater recharge estimation using tritium tagging method. *Proc. Indian Natl. Sci. Acad., Part A*, 1980, **46**, 84–98.
11. APHA, Standard methods for the examination of water and waste water. American Public Health Association, Washington DC. 2005, 21st edn.
12. Maurya, A. S., Shah, M., Deshpande, R. D., Bhardwaj, R. M., Prasad, A. and Gupta, S. K., Hydrograph separation and precipitation source identification using stable water isotopes and conductivity: River Ganga at Himalayan foothills. *Hydrol. Process*, 2010, doi: 10.1002/hyp.7912.
13. Bureau of Indian Standards, Drinking water specification. 1991, IS:10500:1991.
14. World Health Organisation, Guidelines for drinking-water quality incorporating first addendum to Third Edition. WHO, Recommendations, Geneva, 2008, vol. 1.
15. Davis, J. C., *Statistics and Data Analysis in Geology*, Wiley, Singapore, 2002.
16. Rina, K., Datta, P. S., Singh, C. K. and Mukherjee, S., Characterization and evaluation of processes governing the groundwater quality in parts of the Sabarmati basin, Gujarat using hydrochemistry integrated with GIS. *Hydrol. Process*, 2011, doi: 10.1002/hyp.8284.
17. Datta, P. S., Bhattacharya, S. K. and Tyagi, S. K., ^{18}O studies on recharge of phreatic aquifers and groundwater flow-paths of mixing in the Delhi area. *J. Hydrol*., 1996, **176**, 25–36.
18. Rajmohan, N. and Elango, L., Identification and evolution of hydrogeochemical processes in the groundwater environment in an area of the Palar and Cheyyar River Basins, southern India. *Environ. Geol*., 2004, **46**, 47–61.
19. Vengosh, A. and Rosenthal, E., Saline groundwater in Israel: its bearing on the water crisis in the country. *J. Hydrol.*, 1994, **156**, 389–430.
20. Vengosh, A. and Ben-Zvi, A., Formation of a salt plume in the coastal plain aquifer of Israel: the Be'er Toviyya region. *J. Hydrol*., 1994, **160**, 21–52.
21. Vengosh, A., Gill, J., Davisson, M. L. and Hudson, G. B., A multiisotope (B, Sr, O, H and C) and age dating study of groundwater from Salinas Valley, California: hydrochemistry, dynamics, and contamination process. *Water Resour. Res*., 2002, **38**, 1–17.
22. Metcalf & Eddy Inc., Integrated Aquifer Management Plan: Final Report. Gaza Coastal Aquifer Management Program, 2000.
23. Mondal, N. C., Singh, V. P., Singh, V. S. and Saxena, V. K., Determining the interaction between groundwater and saline water through groundwater major ions chemistry. *J. Hydrol*., 2010, **388**, 100–111.
24. Ghabayen, S. M. S., McKee, M. and Kemblowski, M., Ionic and isotopic ratios for identification of salinity sources and missing data in the Gaza aquifer. *J. Hydrol.*, 2006, **318**, 360–373.
25. Gupta, S. K. and Deshpande, R. D., Groundwater isotopic investigations in India: what has been learned? *Curr. Sci.*, 2005, **89**, 825–835.
26. Agarwal, M., Gupta, S. K., Deshpande, R. D. and Yadava, M. G., Helium, radon and radiocarbon studies on a regional aquifer system of the North Gujarat–Cambay region, India. *Chem. Geol.*, 2006, **228**, 209–232.
27. Piper, A. M., A graphic procedure in the chemical interpretation of water analysis. *Am. Geophys. Union Trans*., 1944, **25**, 914–923.
28. Schoeller, H., Qualitative evaluation of groundwater resource. In *Methods and Techniques of Ground-water Investigation and Development*, UNESCO, 1965, pp. 54–83.
29. Appelo, C. A. J. and Postma, D., *Geochemistry, Groundwater and Pollution*, Balkema, Rotterdam, 1994, p. 536.
30. Todd, D. K., *Groundwater Hydrology*, Wiley, New York, 1980.
31. Domenico, P. A. and Schwartz, F. W., *Physical and Chemical Hydrogeology*, Wiley, New York, 1990.
32. US Salinity Laboratory Staff, Diagnosis and improvement of saline and alkaline soils. USDA handbook 60, USDA, Washington, 1954.

ACKNOWLEDGEMENTS. We thank the anonymous reviewers for valuable suggestions. We also thank Dr S. K. Tyagi, NRL, Pusa for help in water analysis and Dr R. D. Deshpande, Physical Research Laboratory (PRL), Ahmedabad, for his support in isotopic analysis in a laboratory at PRL set up under the National Programme on Isotope Fingerprinting of Waters of India, funded jointly by DST, New Delhi and PRL.

Received 8 March 2012; revised accepted 7 January 2013